Time-Domain Electromagnetic Analysis of Interconnects in a Computer Chip Package

Wiren D. Becker, *Student Member, IEEE*, Paul H. Harms and Raj Mittra, *Fellow, IEEE*

Abstract—**The determination of an equivalent circuit to approximate the behavior of an interconnect in a computer package is an important step in the performance evaluation of a computer. Equivalent circuits allow the analysis of a complete interconnect path in a circuit simulator where a full-wave analysis tool would require more memory or computer time than in currently available. Two important components of an interconnect in a computer package are uniform transmission lines, such as a microstrip line or a stripline, and a discontinuity in the interconnect, such as via between two transmission lines. This paper presents a methodology for deriving a frequency-dependent description of coupled transmission lines and equivalent circuit of a via using time-domain full-wave solutions of Maxwell's equations.**

I Introduction

THE DESIGN of present day digital computers requires the electrical characterization of the interconnection circuits that exist in the computer package to ensure reliable and predictable performance of the computer. Accurate timing analysis of the electrical signals and accurate determination of the minimum logic levels at a receiver are two important parameters that need to be determined when designing the computer. Discontinuities along the interconnect path introduce a time delay and cause reflections that affect the signal delay and the transient logic levels of a digital circuit, possibly causing erroneous behavior of the computer [1].

Portions of a computer package interconnect may have a uniform cross-section transverse to the direction of propagation such as a microstrip line or a stripline. The transmission line parameters to be determined are the frequency-dependent inductance and capacitance matrices or, equivalently, the frequency-dependent modal impedances and propagation delays of the uniform transmission lines. A methodology for determining the frequency-dependent parameters of a transmission lines is illustrated by using the finite difference time domain (FDTD) method [2] to analyze a microstrip line and a coupled microstrip line. Once the transmission line parameters are determined, the uniform portions of the interconnects may be modeled in transmission line simulators such as the one described by Blazeck and Mittra [3] or transmission line models included in SPICE or ASTAP.

Manuscript received March 31, 1992; revised August 3, 1992.

The authors are with the Electromagnetic Communication Laboratory. University of Illinois at Urban-Champaign, Urbana, IL 61801.

IEEE Log Number 9203691.

When a uniform transmission line is interrupted, a reflection occurs and additional delay is introduced. This interruption is referred to as a discontinuity in the interconnect path. The discontinuity is most easily modeled in a circuit simulator using a lumped circuit model consisting of inductance, capacitance, and resistance. This paper investigates the reflection from a via in a interconnect path and presents a methodology for determining an equivalent circuit that may be included with the transmission line models in the circuit simulators. Two via geometries are presented: a rectangular via passing through a pair of ground planes, and a cylindrical via passing through a hole in a ground plane coated on both sides by a dielectric slab. The rectangular via is analyzed using two time-domain electromagnetic field algorithms: finite difference time domain (FDTD) [2] and transmission line matrix (TLM) [4]. The cylindrical via is analyzed using a nonorthogonal FDTD technique [5], [6]. The electromagnetic waveforms obtained using these solvers are used to determine the scattering parameters of the vias from which equivalent circuits are derived.

The use of FDTD or TLM provides a full-wave analysis tool for determining the electromagnetic field behavior of the interconnect components. The FDTD and TLM algorithms allow the modeling of arbitrarily shaped material regions which compose an interconnect path since the computational space is discretized into cells where the material properties of each cell can be specified. Time-domain analysis allows the efficient determination of frequency-dependent parameters through the use of the Fourier transform.

The equivalent circuit allows the designer to approximate the behavior of the discontinuity in a circuit simulator where complex transmission line circuits with nonlinear terminations can be included. An interconnect with numerous path discontinuities and distributed nonlinear loads can be analyzed in a general circuit simulator.

II. Uniform Transmission Lines

A uniform transmission line refers to a constant cross-section guided-wave structure such as a microstrip line or stripline. The materials that comprise the cross-section need not be homogeneous or constant along the two-dimensional cross-section, but the cross-section must be the same at any point along the line. In this environment, the propagation delay and the impedance will be functions of

frequency. This section describes a systematic and accurate method of determining these frequency-dependent parameters using the FDTD algorithm.

A. Approach

Zhang *et al.* [7] have discussed the effect of the imperfectly absorbing boundaries on the calculation of the transmission line impedance and propagation constant due to the sensitivity of the Fourier transform results to reflections from the boundaries. Several methods for reducing the undesired reflection have been presented. In [7], Zhang *et al.* solved the problem by running the FDTD solver twice, once terminating the FDTD mesh with magnetic walls, and once with electric walls, and averaging the results. Zhang and Mei [8] implemented an absorbing boundary condition which provided local cancellation of the leading order errors to minimize the unwanted reflection. Moore and Ling [9] studied a shielded microstrip bend where the structure length was extended as the FDTD simulation progressed so the non-zero electric and magnetic fields would not reach the FDTD mesh boundaries. Bi *et al.* [10] proposed using a dispersive boundary condition which reduces the reflection by absorbing waves composed of multiple phase velocities.

The methodology followed for this paper is to acknowledge the terminating boundary has some reflection and factor that into the analysis. The portion of the wave reflected from the end of the transmission line is treated as an unknown and determined explicitly. Note that this accounts for the reflection from the far wall of a transmission line system, but does not account for the reflection from the side walls or top cover if an imperfectly absorbing boundaries are used there.

The starting point is to assume the voltages and currents on the transmission line simulated by the FDTD algorithm are the superposition of two traveling steady-state sine waves, a forward wave due to the excitation source and a backward wave from the terminating boundary. Assuming the second reflection from the source boundary is negligible, the voltage and current variation along the line is described by the equation

$$f(z, k) = \Re[Ae^{j\omega k\Delta t}e^{-j\beta z}(1 + \Gamma e^{j2\beta z})] \tag{1}$$

where the amplitude of the incident wave, A, and the reflection coefficient, Γ, are complex unknowns, and the propagation constant, β, is a real unknown when a lossless transmission line is considered. The $\Re[\cdot]$ operator takes the real part of the expression. The variable, k, is the time stepping index from FDTD and Δt is the time between time steps k and $k + 1$. The impedance of the transmission line is determined from the ratio of the amplitudes of the incident voltage and current waveforms

$$Z_0(\omega) = \frac{A_{\text{voltage}}}{A_{\text{current}}}, \tag{2}$$

and the effective dielectric constant is determined from the propagation constant as

$$\epsilon_{\text{reff}}(\omega) = \left(\frac{\beta c}{\omega}\right)^2 \tag{3}$$

where c is the speed of light in air.

This problem is similar to a slotted transmission line problem with fixed measurement points. However, in a slotted line measurement, only the power at each measurement point is known. Here, the time record is known so it is possible to determine the five unknowns from one analysis. By multiplying both sides of (1) by sin (ωt) dt and integrating over the time duration of the FDTD run and then multiplying both sides by cos (ωt) dt and integrating over the same time duration, two independent, real equations for each measurement point are generated. Since there are two real equations for each measurement point and a total of five real unknowns, at least three measurement points must be chosen to obtain five independent equations. If more than three points are chosen, the problem is formed into a matrix equation and solved by a least squares procedure.

Although (1) is written in time-harmonic form, the FDTD simulation is performed using a source composed of a band of frequencies. The characteristic impedance and effective dielectric constant are calculated over the desired frequency range by first post-processing the FDTD waveforms to obtain the amplitude and phase information for each frequency at each measurement point. The details of this analysis are shown in the Appendix.

The terminating wall does not need to be an absorbing boundary. This procedure will work with any termination as long as the termination can be described by a lumped parameter model, a single mode exists on the transmission line, and the reflection from the wall at the source end can be neglected.

B. Transmission Line Results

To test this algorithm, the impedance and effective dielectric constant obtained with this method are compared to the results presented by Zhang *et al.* [7]. The microstrip is modeled as outlined in [7]: the strip is 0.15 mm wide and 0.1 mm above the reference plane on a substrate with a relative dielectric constant of 13. A 30 × 55 × 160 cell FDTD mesh with a cell size of $h = 0.0125$ mm in each direction fills the spatial domain and the fields are calculated with a time step of $0.57\ h/c$ seconds where c is the speed of light in free space. The FDTD mesh is terminated by the first-order Mur absorbing boundary condition [11].

The electric field orthogonal to the direction of propagation is excited over the cross-section of the microstrip line at the source end of the microstrip with an amplitude at each electric field point in the cross-section corresponding to the quasi-static electric field of the microstrip line. A Gaussian pulse 250 time steps wide at the five percent

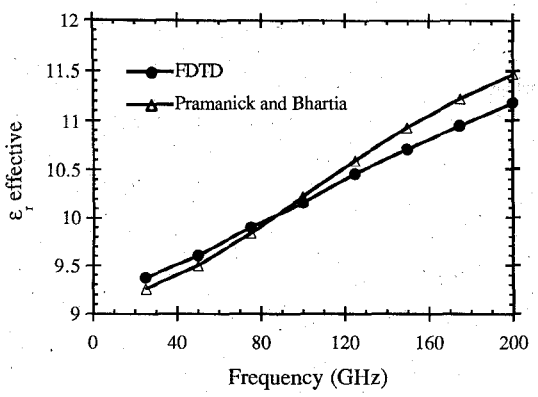

Fig. 1. The effective dielectric constant as a function of frequency for a microstrip line which was also analyzed using FDTD by Zhang *et al.* [7]. The effective dielectric constant calculated using an empirical formula from Pramanick and Bhartia [12] is shown for reference.

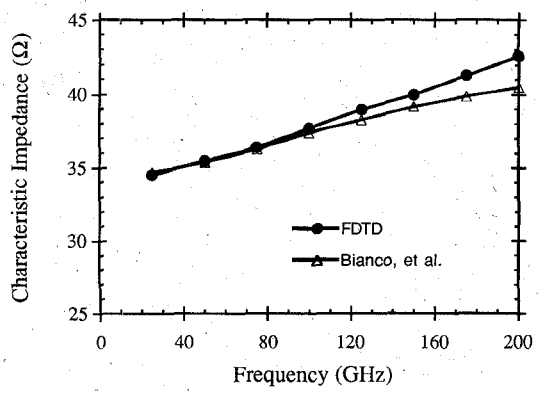

Fig. 2. The characteristic impedance of a microstrip line which was also analyzed in FDTD by Zhang *et al.* [7]. The characteristic impedance calculated using an empirical formula from Bianco *et al.* [13] is shown for reference.

points of the peak amplitude of the pulse is used for the source. Eight measurement points are chosen for monitoring the voltages and currents on the line: from $z = 45$ h to 150 h in 15 h increments. The least squares procedure outlined in the Appendix is then applied to determine the impedance and propagation characteristics of the microstrip line.

The effective dielectric constant is shown graphically in Fig. 1 along with the result obtained using an empirical formula from Pramanick and Bhartia [7 (Fig. 5), 12] for frequencies between 25 and 200 GHz. The characteristic impedance is shown in Fig. 2 and compared to the an empirical formula from Bianco *et al.* [7 (Fig. 6), 13]. For the impedance calculation, the voltage is defined as the averaged line integral of the vertical electric field under the whole strip as was done in [7]. The effective dielectric constant and characteristic impedance of Figs. 1 and 2 compare very closely with the FDTD results published in [7].

In many computer package applications the transmission lines are placed closely enough to each other to significantly impact signal propagation. As an example, consider the shielded coupled microstrip line shown in Fig. 3. A pair of strips are place on a substrate 0.25 mm thick with a relative dielectric constant of 4.5. The strips have a width of 0.30 mm and a thickness of 0.05 mm, and are separated by 0.30 mm. The side walls and top cover are modeled as perfectly conducting walls forming a box that is 4.0 by 1.2 mm in cross-section. The even and odd mode impedances are determined by using the symmetry of the problem and solving the problem twice: once with a electric wall midway between the strips for the odd mode and once with a magnetic wall between the strips for the even mode.

A Gaussian pulse is used for the source, and six measurement points each placed 1.5 mm apart are chosen. The effective relative dielectric constants obtained using the fitting procedure are shown over the frequency range of 5 to 25 GHz in Fig. 4 for the even and odd mode. The relative dielectric constant of an isolated single strip is also plotted in Fig. 4 for reference. The single line and

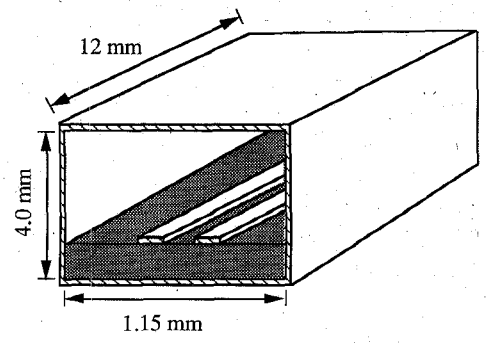

Fig. 3. The coupled microstrip line. The strips are 0.05 by 0.3 mm and separated by 0.3 mm, the dielectric slab is 0.25 mm thick and has a relative dielectric constant ϵ_r, of 4.5.

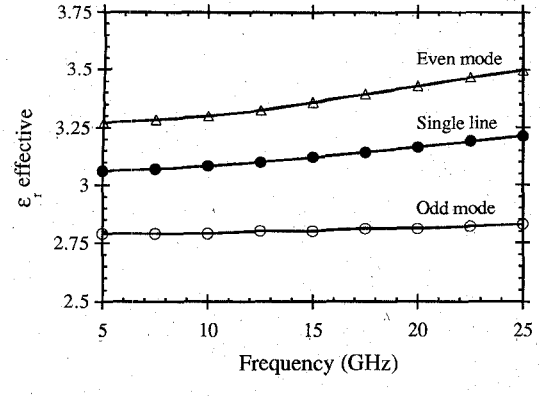

Fig. 4. The effective dielectric constant for the coupled microstrip line of Fig. 3. The effective dielectric constants for the even mode, odd mode, and a single line are shown.

even and odd mode impedances are shown in Fig. 5. As can be seen in Figs. 4 and 5, the even mode exhibits a greater frequency dependence than the odd mode or single line.

As will be seen in the next section, the transmission lines presented above are also useful for analyzing interconnects with discontinuities, e.g. a via. It may also be worthwhile to mention that the method presented herein is applicable to a general transmission line configuration which can be arbitrarily inhomogeneous.

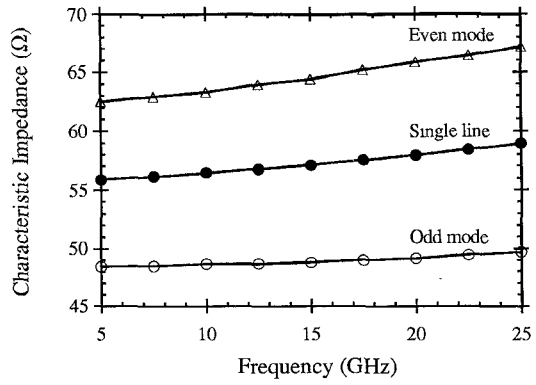

Fig. 5. The characteristic impedance of the coupled microstrip line of Fig. 3. The characteristic impedance for the even mode, odd mode, and a single line are shown.

III. The Via

A via, the portion of an interconnect providing a electrical path between uniform transmission lines on two levels of a package, is a discontinuity on an interconnect path. Two vias are analyzed using FDTD or TLM and an equivalent circuit consisting of inductance and capacitances is obtained for each. The first via is one which fits a rectangular grid and connects a stripline on one level and passes through two ground planes to a stripline on another level. The second is a cylindrical via which connects a microstrip on one side of a dielectric coated ground plane to a microstrip on the other side.

A. Approach

The first step in determining the equivalent circuit parameters for the via is to employ a time-domain Maxwell solver, e.g., TLM or FDTD, using a Gaussian pulse excitation to obtain the total voltage and current waveforms at the input and output ports from which the scattering parameters are determined. The voltage is determined by integrating the vertical electric field from the strip to the adjacent grounded conductor. The transmission line current is determined by performing a closed line integral of the magnetic field around the strip. The path of the line integral forms a rectangle whose edges coincide with the magnetic field components parallel to the strip one-half cell distance away.

The TEM mode of the stripline is excited near the input port using a spatial distribution of the electric field determined by the solution of Laplace's equation on a finite-difference grid. As outlined below, the calculation of the scattering parameters requires the knowledge of the incident field which is easily determined by exciting a uniform stripline.

The time-domain solver is run for the via structure to obtain the total voltage and current at the input and output ports. The scattering parameters are then determined by a DTFT (discrete-time Fourier transform, denoted below by the $\Im[\cdot]$ operator) of the current or voltage waveforms,

$$F_i(\omega) = \Im[f_i(k)] = \sum_{k=0}^{N-1} f_i(k)e^{-j\omega k} \tag{4}$$

where $f_i(k)$ is the time series output of the current or voltage at port i ($i = 1$ (input) or 2 (output)) and $F_i(\omega)$ is the Fourier transform of $f_i(k)$. The frequency-dependent scattering parameters are then calculated by

$$S_{11}(\omega) = \frac{F_{\text{refl}}(\omega)}{F_{\text{inc}}(\omega)} \tag{5}$$

$$S_{21}(\omega) = \frac{F_2(\omega)}{F_{\text{inc}}(\omega)} \tag{6}$$

where $F_{\text{inc}}(\omega)$ is the transform of the incident voltage or current as computed using (4), and $F_{\text{refl}}(\omega)$ is the Fourier transform of the reflected waveform given by

$$F_{\text{refl}}(\omega) = \Im[f_1(k) - f_{\text{inc}}(k)]. \tag{7}$$

Once the scattering parameters for the via are determined, an equivalent circuit model may be obtained by using TouchStone [14]. TouchStone has an optimizing feature that allows the elements of a given circuit to be fitted to a set of given scattering parameters.

To complete the analysis, the circuit model is analyzed by the time domain circuit simulator, Multiple Transmission Line Time Domain Analysis (MTLTDA), which is described by Blazeck and Mittra [3]. MTLTDA is a circuit simulator that allows multiple lossy transmission lines with frequency-dependent inductance and capacitance matrices and nonlinear terminations. For these via structures, however, only a single lossless transmission line with linear discrete elements is needed.

B. Rectangular Via Results

The via chosen for analysis is shown in Fig. 6. The stripline cross-section measures 0.25 millimeters by 1.25 millimeters and the ground planes are placed so the impedance of the stripline is approximately 50 ohms. The via has a rectangular cross section of 0.50 millimeters by 0.75 millimeters which fits the rectangular grid used in the time-domain analysis. The fields on the walls at the input and output ports are determined using the first order Mur absorbing boundary condition.

The FDTD and TLM mesh is comprised of cells 0.250 millimeters (h) on a side, and a time step (Δt) of 0.417 ps ($\Delta t = h/2c$) where c is the speed of light in free space. The temporal variation of the excitation pulse is a Gaussian distribution with a width of 60 time steps (25 ps). This pulse has a 3 dB cutoff frequency of approximately 20 GHz. The voltages and currents are monitored at the input and output ports which are thirty cells (7.5 mm) from the center of the via.

After the time-domain solvers are run, the time variation of the voltages and currents at the input and output ports are available. The time-domain voltage waveforms from the TLM analysis at the input and output port are shown in Fig. 7. The scattering parameters are then calculated as outlined in the previous section. The magnitudes of the scattering parameters, $S_{11}(\omega)$ and $S_{21}(\omega)$, are shown in Fig. 8 for frequencies up to 20 GHz as calculated using the voltage waveforms from TLM and FDTD.

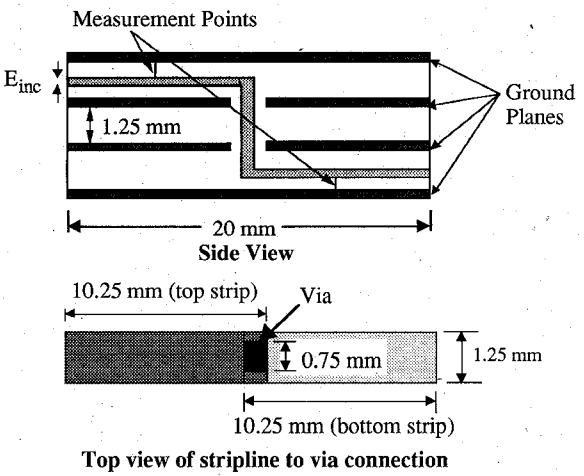

Fig. 6. The rectangular via connecting two striplines on different levels in a multilayer circuit board configuration. The striplines are 0.25 mm by 1.25 mm, the via is 0.5 by 0.75 mm, and the ground planes are separated from the via by 0.25 mm.

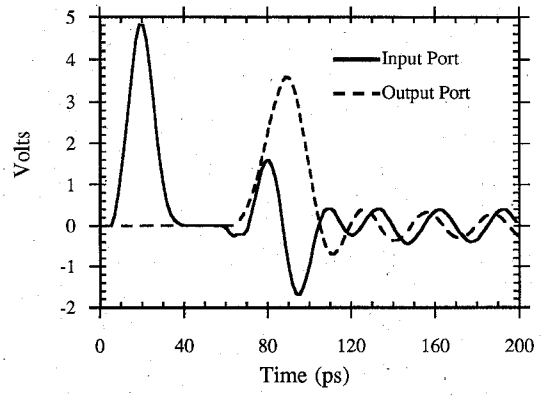

Fig. 7. The first 200 ps of the time-domain TLM voltage waveform of the rectangular via at the input and output ports.

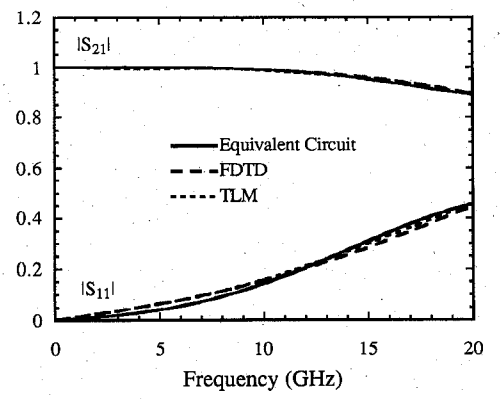

Fig. 8. The magnitude of the rectangular via scattering parameters. The scattering parameters of the equivalent circuit (Fig. 9) are shown along with those determined by FDTD and TLM.

The circuit model shown in Fig. 9 represents the via structure of Fig. 6. Note that the striplines have been modeled as ideal transmission lines; the stripline to via transition regions have been represented by a lumped Π-circuit consisting of C_1, C_2 and L_1; and the via portion between the middle two planes has been modeled by L_2.

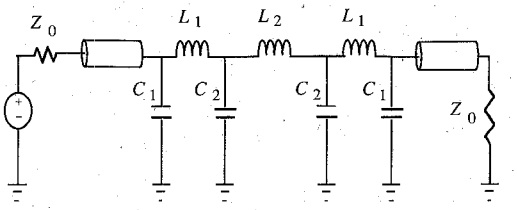

Fig. 9. The equivalent circuit chosen to represent the rectangular via discontinuity. The transmission lines represents the stripline portions and the inductors and capacitors represent various parts of the via. The element values are $Z_0 = 48.5$, $C_1 = 0.119$ pF, $C_2 = 0.075$ pF, $L_1 = 0.470$ nH, $L_2 = 0.062$ nH as determined by TouchStone.

In TouchStone the scattering parameters of the equivalent circuit are matched to the Fourier-transformed time domain results for the frequencies ranging from 0.48 GHz to 20 GHz. The element values to achieve this fit are: $C_1 = 0.119$ pF, $C_2 = 0.075$ pF, $L_1 = 0.47$ nH, $L_2 = 0.062$ nH. The magnitudes of the scattering parameters of the equivalent circuit are plotted in Fig. 8 along with the scattering parameters obtained using FDTD and TLM. TouchStone matches S_{11} well in the middle of the 0.48 to 20 GHz spectrum, but some error arises at the low and high end of that frequency spectrum. S_{21} is well-matched throughout the spectrum.

The final step is to place the equivalent circuit model into the time domain transmission line simulator MTLTDA [3]. At 35.3 GHz, the side walls and ground planes in the TLM simulation form a waveguide which supports a TE_{10} mode. Even though the Gaussian pulse has a 3 dB frequency of 20 GHz, there is still a considerable amount of power in the pulse above 35.3 GHz. The equivalent circuit does not take into account the excitation of the waveguide mode, and the Gaussian waveform is approximated by a trapezoidal pulse in MTLTDA so a direct comparison between the two waveforms does show some differences. However, by passing the time-domain waveforms through a Hanning low-pass filter to remove the frequency components above 20 GHz, the equivalence of the time-domain voltage response becomes apparent as shown in Fig. 10 where the filtered TLM waveforms of Fig. 7 are compared to the filtered waveforms from MTLTDA.

C. Cylindrical Via Results

An equivalent circuit model of a cylindrical via discontinuity is obtained using the same procedures as for the rectangular via; however, due to the complicated geometry, the nonorthogonal FDTD technique [5], [6] is employed to perform the time-domain analysis. In this section, the results of the nonorthogonal FDTD computations will be compared with a conventional FDTD analysis [2] and measurements taken from Maeda *et al.* [15]. An equivalent circuit of the via extracted from the scattering parameters will be given.

The cylindrical via discontinuity [15] is shown in Fig. 11. The via diameter is 0.7 mm, its length is 3.2 mm, the pad diameter is 3.9 mm, and the width of the connecting microstrip is 3.3 mm. The dielectric slab is

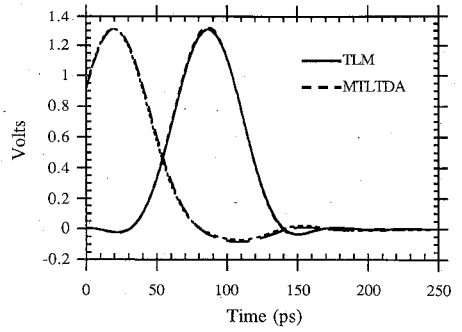

Fig. 10. The time domain TLM and MTLTDA circuit waveforms at the input and output ports after being filtered by a Hanning window with a 20 GHz cutoff frequency.

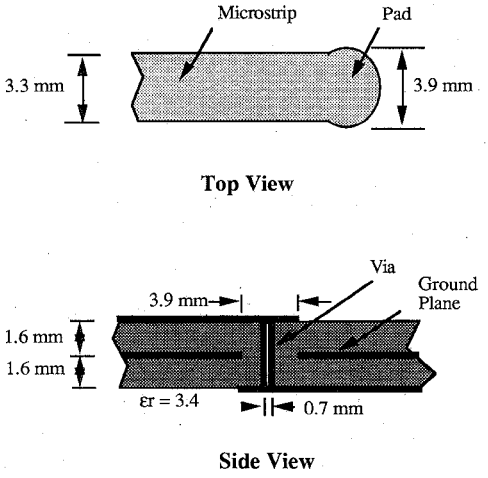

Fig. 11. The geometry of the cylindrical via discontinuity.

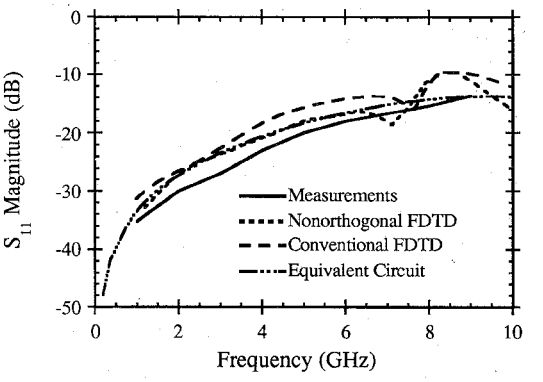

Fig. 12. A comparison of the magnitude of S_{11} computed with the nonorthogonal FDTD time-domain waveforms to the measurements of S_{11} [15].

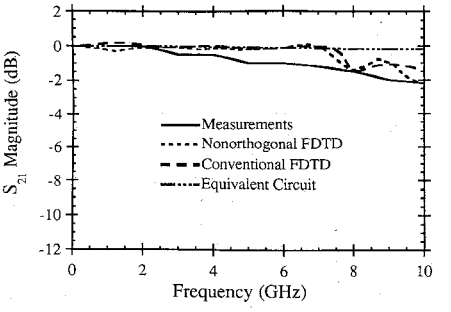

Fig. 13. A comparison of the magnitude of S_{21} computed with the nonorthogonal FDTD time-domain waveforms to the measurements of S_{21} [15].

3.2 mm thick, and its permittivity is 3.4. The ground plane, which is in the center of the slab, has a circular cutout of 3.9 mm in diameter for the via.

The cylindrical via is discretized with a nonorthogonal grid, providing a piecewise linear model of the entire structure. The via was enclosed in a rectangular box with two perfectly conducting (pec) side walls, one pec top and bottom wall and first-order Mur absorbing boundary conditions for the end walls [11]. The absorbing walls were at the near- and far-end of the discontinuity, respectively. The enclosure was 42.04 mm in length by 19.5 mm in width by 16 mm in height. This region was discretized with 8000 nonorthogonal FDTD cells, providing a mesh density of 10 cells per wavelength at 13-14 GHz. For the conventional FDTD calculations, the region was discretized with an orthogonal mesh consisting of 16 470 unit cells with cross-sections of 0.7×0.7 mm^2. For both grids, four cell layers were employed in the dielectric and three layers in each air region above and below the dielectric. A Gaussian pulse with a quasi-TEM modal spatial distribution was used as the excitation.

The scattering parameters were computed from the FDTD results using the FFT and compared with measurements from [15]. Figs. 12 and 13 show agreement between the computations and the measurements up to 7–8 GHz. The nonorthogonal results are either closer to the measurements than the conventional FDTD results or just as good, indicating that the nonorthogonal method—which is based on a grid of 8000 cells—is as accurate as the conventional technique based on a mesh of 16 470 cells. This result shows that the nonorthogonal FDTD technique can model the via as well as the conventional FDTD method with approximately 50% fewer unit cells. The savings in number of cells for a particular problem will depend upon the geometry and required frequency bandwidth. Although not shown here, experiments with other nonorthogonal geometries and an error analysis have shown that the reduction in number of cells relative to the conventional FDTD can be much greater for some problems [16].

The discrepancies between the computed values and the measurements are attributable to two major factors other than the errors in reading the measured results from [15]. One is that the discretizations for both finite-difference meshes become more inaccurate for the higher frequencies because the cell sizes are no longer sufficiently small in comparison with the wavelengths at these frequencies. For this structure, a mesh density of up to 20 or more cells per wavelength of the highest frequency component may be necessary to obtain accurate results over the entire frequency band. The other error stems from the use of pec side, top and bottom walls to truncate both meshes, creating an artificial waveguide surrounding the via which is originally in an open region. The cutoff wavelength of the

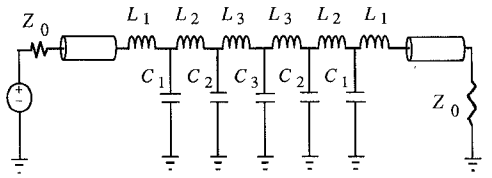

Fig. 14. An equivalent circuit of the cylindrical via discontinuity. The transmission lines have an impedance of 55 ohms, and a effective dielectric constant of 2.76. L_1 = 369.7 pH, L_2 = 5.915 pH, L_3 = 723.17 pH, C_1 = .25283 pF, C_2 = 0.00118 pF and C_3 = 0.3393 pF.

waveguide structure is within the computed frequency range of the via scattering parameters, and the excited modes of the waveguide distort the scattering parameters of the via. In a further study of this problem, the side, top and bottom conducting walls were replaced by first-order Mur absorbing boundary conditions which resulted in improvements in S_{21} over the entire frequency range shown. The form of the numerical results for S_{11} improved, but the low-frequency level became worse for the nonorthogonal analysis. A suitable absorbing boundary condition compatible with the nonorthogonal grid and useful for guided wave problems needs to be implemented.

The equivalent circuit of the cylindrical via discontinuity shown in Fig. 14 was developed from the scattering parameter results obtained from the nonorthogonal FDTD analysis by using the same procedure given for the rectangular via. The equivalent circuit consists of ideal transmission lines for modeling the microstrip lines and a lumped L-C network for modeling the pads and via. This circuit model accurately reproduces the scattering parameter results from the nonorthogonal FDTD analysis up to approximately 6 GHz, as shown in Figs. 12 and 13.

IV. Conclusions

A methodology for determining equivalent circuits of the various components of a computer package interconnect has been demonstrated. The equivalent circuits are suitable for use in circuit simulators or transmission line simulators. The numerous transmission lines and discontinuities that make up an interconnect path may be included in a circuit model to determine the congregate delays and reflections that exist on the interconnect when used in a computer circuit with nonlinear drivers and receivers. The described approach is general in that it can be applied to transmission lines or discontinuities with complex geometric descriptions including many commonly found in multichip computer packages.

To accurately model the curved geometry, the nonorthogonal FDTD algorithm was employed instead of the conventional FDTD method because it provides a piecewise linear model of curved surfaces, and with the variable mesh density it can represent complicated structures without an excessive number of unknowns.

Appendix

In order to determine the characteristic impedance, Z_0, and the propagation constant, β, of a uniform transmission line such as the stripline or microstrip line, it is important to either minimize the effect of the terminating boundary or quantify the effect so the reflection can be removed. The method used in this paper is to start with (1) as a model for the propagation of the voltage or current along the transmission line which includes the reflection from the far boundary. Equation (1) assumes a single steady-state sine wave exists on the line. Taking the real part of the right-hand side of (1) leads to

$$\begin{aligned} f(z, k) &= |A| \cos(\omega k\Delta t - \beta z + \phi_1) \\ &\quad + |A\Gamma| \cos(\omega k\Delta t + \beta z + \phi_2) \\ A &= |A| e^{j\phi_1} \\ \Gamma &= |\Gamma| e^{j(\phi_2 - \phi_1)}. \end{aligned} \tag{A1}$$

Then multiplying both sides by $\sin(\omega t)dt$ and $\cos(\omega t)dt$ and integrating over the $N + 1$ samples of the FDTD run spanning the time $[0, T]$, gives for the left-hand side of (A1)

$$\begin{aligned} \text{L.H.S.} &= \int_0^T f(z, k) \begin{Bmatrix} \sin(\omega t) \\ \cos(\omega t) \end{Bmatrix} dt \\ &= \sum_{k=0}^{N} f(z, k) \begin{Bmatrix} \sin(\omega k\Delta t) \\ \cos(\omega k\Delta t) \end{Bmatrix} \Delta t \end{aligned} \tag{A2}$$

by the trapezoidal rule of integration. The right-hand side of (A1) after using trigonometeric identities is

$$\begin{aligned} \text{R.H.S.} &= \cos(\beta z)[|A| \cos(\phi_1) \\ &\quad + |A\Gamma| \cos(\phi_2)] \int_0^T \begin{Bmatrix} \sin(\omega t)\cos(\omega t) \\ \cos^2(\omega t) \end{Bmatrix} dt \\ &\quad + \sin(\beta z)[|A| \sin(\phi_1) \\ &\quad - |A\Gamma| \sin(\phi_2)] \int_0^T \begin{Bmatrix} \sin(\omega t)\cos(\omega t) \\ \cos^2(\omega t) \end{Bmatrix} dt \\ &\quad + \sin(\beta z)[|A| \cos(\phi_1) \\ &\quad - |A\Gamma| \cos(\phi_2)] \int_0^T \begin{Bmatrix} \sin^2(\omega t) \\ \sin(\omega t)\cos(\omega t) \end{Bmatrix} dt \\ &\quad + \cos(\beta z)[-|A| \sin(\phi_1) \\ &\quad - |A\Gamma| \sin(\phi_2)] \int_0^T \begin{Bmatrix} \sin^2(\omega t) \\ \sin(\omega t)\cos(\omega t) \end{Bmatrix} dt. \end{aligned} \tag{A3}$$

Equations (A2) and (A3) are evaluated twice at each measurement point, first with the upper terms in the { } brackets and then with the bottom terms. To simplify the notation, let

$$a = \int_0^T \cos^2(\omega t)\, dt = \frac{T}{2} + \frac{1}{4\omega} \sin(2\omega T) \tag{A4}$$

$$b = \int_0^T \cos(\omega t) \sin(\omega t)\, dt = \frac{1}{2\omega} \sin^2(\omega T) \tag{A5}$$

$$c = \int_0^T \sin^2(\omega t)\, dt = \frac{T}{2} - \frac{1}{4\omega}\sin(2\omega T). \quad \text{(A6)}$$

The problem can now be written as a matrix equation of the form $A(\beta) \cdot x = b$ where x is a 4×1 vector which includes four of the unknowns ($|A|$, $|\Gamma|$, ϕ_1, and ϕ_2),

$$x = \begin{bmatrix} |A|\cos(\phi_1) + |A\Gamma|\cos(\phi_2) \\ |A|\sin(\phi_1) - |A\Gamma|\sin(\phi_2) \\ |A|\cos(\phi_1) - |A\Gamma|\cos(\phi_2) \\ -|A|\sin(\phi_1) - |A\Gamma|\sin(\phi_2) \end{bmatrix} \quad \text{(A7)}$$

and the fifth unknown, β, is included in the matrix A where p is the number of measurement points in the FDTD run.

A is a $2p \times 4$ matrix,

$$A = \begin{bmatrix} a\cos(\beta z_1) & a\sin(\beta z_1) & b\sin(\beta z_1) & b\cos(\beta z_1) \\ b\cos(\beta z_1) & b\sin(\beta z_1) & c\sin(\beta z_1) & c\cos(\beta z_1) \\ \vdots & \vdots & \vdots & \vdots \\ a\cos(\beta z_p) & a\sin(\beta z_p) & b\sin(\beta z_p) & b\cos(\beta z_p) \\ b\cos(\beta z_p) & b\sin(\beta z_p) & c\sin(\beta z_p) & c\cos(\beta z_p) \end{bmatrix}, \quad \text{(A8)}$$

and b is a $2p \times 1$ vector,

$$b = \begin{bmatrix} \sum_{k=0}^{N} f(z_1, k)\cos(\omega k\Delta t)\,\Delta t \\ \sum_{k=0}^{N} f(z_1, k)\sin(\omega k\Delta t)\,\Delta t \\ \vdots \\ \sum_{k=0}^{N} f(z_p, k)\cos(\omega k\Delta t)\,\Delta t \\ \sum_{k=0}^{N} f(z_p, k)\sin(\omega k\Delta t)\,\Delta t \end{bmatrix}. \quad \text{(A9)}$$

Since the amplitude and phase of the sine wave component is already known from the FDTD run, the integral in (A2) may be solved analytically

$$\int_0^T f(z_i, k) \begin{Bmatrix} \sin(\omega t) \\ \cos(\omega t) \end{Bmatrix} dt = \begin{Bmatrix} b\cos(\theta_i) + a\sin(\theta_i) \\ c\cos(\theta_i) + b\sin(\theta_i) \end{Bmatrix} \quad \text{(A10)}$$

where a, b, and c are (A4), (A5), and (A6), respectively. Furthermore, since steady-state has been reached the results are just as valid if the FDTD time sample covers an integer number of periods of the sinusoidal waveform. In that case,

$$a = c = \frac{T}{2}; \quad b = 0 \quad \text{(A11)}$$

and the matrix equation $(A(\beta) \cdot x = b)$ to solve reduces to

$$\begin{bmatrix} \cos(\beta z_1) & \sin(\beta z_1) & 0 & 0 \\ 0 & 0 & \sin(\beta z_1) & \cos(\beta z_1) \\ \vdots & \vdots & \vdots & \vdots \\ \cos(\beta z_p) & \sin(\beta z_p) & 0 & 0 \\ 0 & 0 & \sin(\beta z_p) & \cos(\beta z_p) \end{bmatrix} \cdot x = \begin{bmatrix} W_1\sin(\theta_1) \\ W_1\cos(\theta_1) \\ \vdots \\ W_p\sin(\theta_p) \\ W_p\cos(\theta_p) \end{bmatrix} \quad \text{(A12)}$$

where x is (A7) and W_i, $i = [1, 2, \cdots, p]$, is the amplitude of the sine wave with relative phase θ_i. The error

$$\text{error} = \|Ax - b\|_2, \quad \text{(A13)}$$

is minimized, where $\|\cdot\|_2$ is the vector 2-norm.

The space variable z_i, $i = [1, 2, \cdots, p]$, denotes the discrete points along the line where the voltage or current is monitored. Since β appears in the matrix A, the problem is nonlinear. The method chosen to solve this system of equations was an iterative process where an initial β is chosen, and the vector, x, is determined using the linear least squares method. The downhill simplex method of Nelder and Mead [17] yields an updated estimate of β. These two steps are repeated until the error criterion (A13) is minimized.

Once the error is minimized, the iterative procedure is terminated and β is known from the final value chosen in the iterative loop. The other four unknowns are determined by the manipulation of the final x vector:

$$y = \frac{1}{2}\begin{bmatrix} 1 & 0 & 1 & 0 \\ 1 & 0 & -1 & 0 \\ 0 & -1 & 0 & -1 \\ 0 & 1 & 0 & -1 \end{bmatrix} x = \begin{bmatrix} |A|\cos(\phi_1) \\ |A\Gamma|\cos(\phi_2) \\ |A\Gamma|\sin(\phi_2) \\ |A|\sin(\phi_1) \end{bmatrix}, \quad \text{(A14)}$$

$$|A| = \sqrt{y(1)^2 + y(4)^2}, \quad (15)$$

$$|\Gamma| = \frac{\sqrt{y(2)^2 + y(3)^2}}{|A|}, \quad (16)$$

$$\phi_1 = \tan^{-1}\left(\frac{y(4)}{y(1)}\right), \tag{17}$$

and

$$\phi_2 = \tan^{-1}\left(\frac{y(3)}{y(2)}\right). \tag{18}$$

This procedure is extended to multiple frequencies by exciting the FDTD mesh with a pulse containing a band of frequencies, such as a Gaussian pulse. The amplitude, W_i, and phase θ_i, for a particular frequency are obtained at each monitoring point z_i, along the transmission line by a Fourier transformation. The above minimization procedure is then applied at each frequency and the frequency variation of the characteristic impedance and effective dielectric constant is obtained using (2) and (3).

Acknowledgment

The authors would like to thank the National Center for Supercomputing Applications (NCSA) for the grant of supercomputer time used to obtain results presented in this paper.

References

[1] E. E. Davidson and G. A. Katopis, "Package electrical design," *Microelectronics Packaging Handbook*, R. R. Tummala and E. J. Rymaszewski, Eds., New York: Van Nostrand Reinhold, 1989, ch. 3.

[2] K. S. Yee, "Numérical solution of initial boundary value problems involving Maxwell's equations in isotropic media," *IEEE Trans. Antennas Propagat*, vol. AP-14, no. 5, pp. 302–307, May 1966.

[3] T. S. Blazeck and R. Mittra, "Transient analysis of lossy multiconductor transmission lines in nonlinear circuits," *IEEE Trans. Comp., Hybrids, Manuf. Technol.*, vol. CHMT-14, no. 3, pp. 618–627, Sept. 1991.

[4] P. B. Johns, "A symmetrical condensed node for the TLM method," *IEEE Trans. Microwave Theory Tech.*, vol. MTT-35, no. 4, pp. 370–377, Apr. 1987.

[5] J.-F. Lee, R. Palandech and R. Mittra, "Modeling three-dimensional discontinuities in waveguides using nonorthogonal FDTD algorithm," *IEEE Trans. Microwave Theory Tech.*, vol. 40, pp. 346–352, Feb. 1992.

[6] M. Fusco, "FDTD algorithm is curvilinear coordinates," *IEEE Trans. Antennas Propagat.*, vol. AP-38, no. 1, pp. 76–89, Jan. 1990.

[7] X. Zhang, J. Fang, K. K. Mei and Y. Liu, "Calculations of the dispersive characteristics of microstrips by the time-domain finite differences method," *IEEE Trans. Microwave Theory Tech.*, vol. 36, no. 2, pp. 263–267, Feb. 1988.

[8] X. Zhang and K. K. Mei, "Time-domain finite-difference approach to the calculation of the frequency-dependent characteristics of microstrip discontinuities," *IEEE Trans. Microwave Theory Tech.*, vol. 36, no. 12, pp. 1775–1787, Dec. 1988.

[9] J. Moore and H. Ling, "Characterization of a 90° microstrip bend with arbitrary miter via the time-domain finite difference method," *IEEE Trans. Microwave Theory Tech.* vol. 38, no. 4, pp. 405–410, Apr. 1990.

[10] Z. Bi, K. Wu, C. Wu, and J. Litva, "A dispersive boundary condition for microstrip component analysis using the FD-TD method," *IEEE Trans. Microwave Theory Tech.*, vol. 40, pp. 774–777, Apr. 1992.

[11] G. Mur, "Absorbing boundary conditions for the finite-difference approximation of time-domain electromagnetic-field equations," *IEEE Trans. Electromagn. Compat.*, vol. EMC-23, pp. 377–382, Nov. 1981.

[12] P. Pramanick and P. Bhartia, "An accurate description of dispersion in microstrip," *Microwave J.*, pp. 89–96, Dec. 1983.

[13] K. C. Gupta, R. Grag, and R. Chadha, *Computer-Aided Design of Microwave Circuits*. Dedham, MA: Artech House, 1981.

[14] TouchStone, EEsof, Inc., 5795 Lindero Canyon Rd., Westlake Village, CA 91362.

[15] S. Maeda, T. Kashiwa and I. Fukai, "Full wave analysis of propagation characteristics of a through hole using the finite-difference time-domain method," *IEEE Trans. Microwave Theory Tech.*, vol. 39, no. 12, pp. 2154–2159, Dec. 1989.

[16] P. H. Harms, J.-F. Lee, and R. Mittra, "A study of the nonorthogonal FDTD method versus the conventional FDTD technique for computing resonant frequencies of cylindrical cavities," *IEEE Trans. Microwave Theory Tech.*, vol. 40, no. 4, pp. 741–746, April 1992.

[17] J. A Nedler, and R. Mead, "A simplex method for function minimization," *The Computer J.* vol. 7, no. 4, pp. 308–313, Jan. 1965.

Wiren D. Becker (S'90) received the B.E.E. degree from the University of Minnesota in 1982 and the M.S.E.E. degree from Syracuse University in 1985.

He joined IBM, East Fishkill, NY in 1982 where he has been involved in research and development of multichip computer packages. He is currently working towards his Ph.D. degree at the University of Illinois at Urbana-Champaign in IBM's Resident Work Study Program. His research interests include the electromagnetic modeling and characterization of electronic packages.

Mr. Becker is a member of Tau Beta Pi.

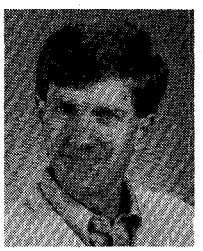

Paul H. Harms received the B.E.E. degree in Electrical Engineering from the Georgia Institute of Technology in 1984, the M.S. degree in Electrical Engineering from the University of Illinois in 1987 and the Ph.D. degree in Electrical Engineering from the University of Illinois in 1992. His present interests are in the numerical and experimental electromagnetic analysis of passive microwave components and electronic packaging.

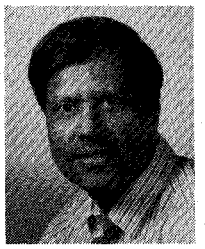

Raj Mittra (S'54–M'57–SM'69–F'71) is Director of the Electromagnetic Communication Laboratory of the Electrical and Computer Engineering Department and Research Professor of the Coordinate Science Laboratory at the University of Illinois. He is a former president of AP-S, and he has served as the editor of the IEEE TRANSACTIONS ON ANTENNAS AND PROPAGATION. He is president of RM Associates, a consulting organization providing services to several industrial and governmental organizations.

Dr. Mittra's professional interests include the areas of analytical and computer-aided electromagnetics, high-speed digital circuits, radar scattering, satellite antennas, microwave and millimeter-wave integrated circuits, frequency selective surface, EMP and EMC analysis, and remote sensing.